AJNR

MR of brain radiation injury: experimental studies in cats.

C Hecht-Leavitt, R I Grossman, W J Curran, Jr, J T McGrath, D N Biery, P M Joseph and D F Nelson

MR of Brain Radiation Injury:
Experimental Studies in Cats

Charles Hecht-Leavitt[1, 2]
Robert I. Grossman[1]
Walter J. Curran, Jr.[3]
John T. McGrath[4]
Darryl N. Biery[4]
Peter M. Joseph[1]
Diana F. Nelson[3]

Two of six cats receiving small-field, single-dose, brain irradiation of 35 Gy with 6 MeV photons developed brain abnormalities in the irradiated area on MR images at 6 and 8 months, respectively, after treatment. The lesions were of high intensity on T2-weighted images and did not enhance after IV administration of gadolinium-DTPA. An additional lesion in one of these cats displayed high signal on T2-weighted images and enhanced on T1-weighted images after IV gadolinium-DTPA. Pathologic correlation revealed that the nonenhancing T2-weighted lesions consisted of edema or demyelinated regions without inflammation while the gadolinium-enhanced lesion demonstrated necrosis with inflammatory infiltrate. Focal brain irradiation may produce noninflammatory demyelination and necrosis. These histologic entities may be potentially distinguished on MR with IV gadolinium-DTPA.

Regions of high-signal abnormality, particularly in the white matter on T2-weighted images, have been noted in patients undergoing radiation therapy [1, 2]. It is unclear what these areas represent. Moreover, patients who have been irradiated may have residual or recurrent tumor as well as the effects of systemic or intrathecal chemotherapy, producing high signal on T2-weighted images. This experiment was designed to investigate the MR appearance of radiation changes in cats' brains unencumbered by tumor, surgery, or chemotherapy and to correlate the MR changes with histology. In this model (1) only a small portion of one hemisphere was irradiated to prevent early death from increased intracranial pressure or damage to vital brainstem structures, and (2) gadolinium-DTPA (Gd-DTPA) was used to image breakdown of the blood-brain barrier in the hope of distinguishing radiation-induced noninflammatory demyelination from radiation necrosis.

Materials and Methods

Commercially obtained cats ranging in age from 6 to 12 months old were scanned by CT (GE 8800), using 5-mm thick sections, before and after an IV bolus injection of 2 ml/kg of iothalamate meglumine 60% (Conray 60%, Mallinckrodt, Inc., St. Louis, MO), or diatrizoate meglumine 60% (Angiovist 282, Berlex Laboratories, Inc., Wayne, NJ), or metrizamide (Amipaque, Winthrop-Breon Laboratories, New York, NY) (370 mg I/ml). Anesthesia was accomplished with IV pentobarbital by a veterinary anesthetist. MR scans were obtained on a 1.4-T GE scanner designed for use in animal studies [3]. Axial spin-echo (SE) imaging was performed with TR = 2000 msec and TE = 100 msec (T2-weighted).

Six animals without clinical, CT, or MR evidence of disease were selected for radiation treatment. The head was shaved and a mark placed on the scalp over the mid portion of the bodies of the lateral ventricles as located by CT. The cats then received 35 Gy cranial radiation via a 1.5 × 1.5 cm square portal to the vertex over the right lateral ventricle with 6 MeV photons. Posttreatment MR scans were obtained at 4–6 week intervals. SE scans were obtained as described above. Inversion recovery (IR) scans with TR = 2000 msec and TI = 800 msec (T1-weighted) were obtained before and after bolus injection of 0.1 mM/kg of Gd-

A   **B**
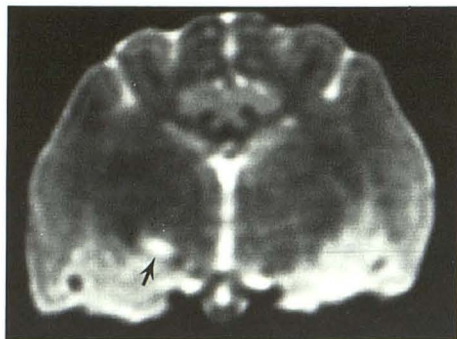
Fig. 1.—MR image of cat A 7 months after irradiation. High-signal lesion (*arrow*) in right cerebral peduncle on T2-weighted image. T1-weighted images were normal before and after Gd. Noninflammatory demyelination. SE 2000/100.
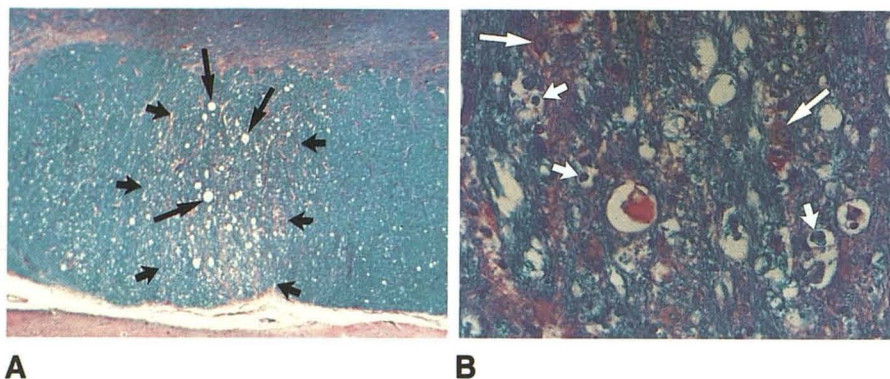
Fig. 2.—Histologic section of right cerebral peduncle of cat A. All illustrated sections stained with H and E, Luxol Fast Blue, and PAS.
  A, Magnification ×30 shows demyelinated lesion as loss of blue color (*short arrows*), prominent vacuolation (*long arrows*).
  B, Same lesion, magnification ×192, shows myelin debris (*short arrows*) and reactive astrocytes (*long arrows*).

DTPA. Two cats showed definite lesions on MR and were sacrificed within 1 week after the lesion became apparent. Before our criteria for MR lesions were well-defined, one cat with a questionable MR lesion was sacrificed at 3 months. One cat died of renal failure secondary to bladder calculi at 5 months without showing MR abnormalities. The two remaining cats were followed for 1 year and then sacrificed. These two cats never showed MR abnormalities. Brains were fixed in formalin and slides prepared from the irradiated tissue and symmetrical areas in the opposite hemisphere. Slides were stained with H and E, Luxol Fast Blue for myelin, and PAS, and interpreted by a veterinary neuropathologist. The pathologic and MR findings were then correlated.

Results

Two cats developed lesions on MR within the irradiated volume. In cat A, a single lesion was identified on MR 7 months after irradiation and manifested as a focal area of high signal on the T2-weighted image in the right cerebral peduncle (Fig. 1). The T1-weighted image, both before and after IV injection of Gd-DTPA, was normal. Histologic section of the right cerebral peduncle showed an area of prominent vacuolation due to the loss of myelin fibers (Fig. 2). Myelin debris was noted within the vacuoles, and astrocytic proliferation was seen as an abundance of astrocytes with increased cytoplasm and enlarged nuclei. No inflammatory cells were seen. A similar but much smaller lesion was seen in the right optic tract but was not in the imaging plane of our MR scans.

In cat B, focal areas of high signal were seen in the periventricular white matter on the right on the T2-weighted images at 8 months (Fig. 3). High signal was also seen extending superiorly and laterally from the ventricle into the subcortical white matter. The area immediately surrounding the ventricle showed enhancement with Gd-DTPA on the T1-weighted image, indicating breakdown of the blood-brain barrier (Fig. 4). Histologic findings immediately above the right lateral ventricle in the corpus callosum and fornix showed tissue necrosis, monocytic infiltration in the wall of the blood vessels, and a suggestion of increased vascularity (Fig. 5).

These are the pathologic changes that identify radiation necrosis [4]. The histologic findings in the areas extending into the subcortical white matter were edema, pallor of the myelin, increased vascularity, and a few reactive astrocytes. No demyelinated axons or myelophages were seen. Necrosis and demyelination were seen in the right optic tract.

The brains of the three cats in which no MR lesions were apparent, and that of the one cat in which there was a questionable MR lesion, were normal by gross and microscopic pathologic examination.

Discussion

Lampert and Davis [5] categorized the adverse clinical effects of cranial irradiation as acute, early delayed, and late delayed. The acute effects, those occurring during the course of irradiation, are thought to be due to vasogenic edema from damage to the capillary endothelium. Early delayed effects, occurring a few weeks to a few months after irradiation, are presumed to be due to demyelination of axons and may be reversible. Early in their course they are associated with inflammatory changes [4]. No studies have yet correlated radiologic findings with pathologically proven acute or early delayed effects. Late delayed effects, occurring months to years later, have been considered radiation necrosis and may be manifest on CT or MR as a mass lesion with surrounding edema and breakdown of the blood-brain barrier [1, 2, 6, 7].

There is controversy as to the mechanisms of injury in each category [8]. In late delayed effects, necrosis is generally thought to be due to ischemia from endothelial proliferation in the microvasculature [4]. The endothelium is the most radiosensitive tissue in the brain. Demyelination may be due to a mechanism similar to necrosis or to direct damage to the oligodendrocyte, which is responsible for maintaining the myelin sheath [9, 10].

Pathologically, radiation necrosis is accompanied by breakdown of the blood-brain barrier [11] and perivascular inflammation [4]. Gd-DTPA has been shown to pass through a
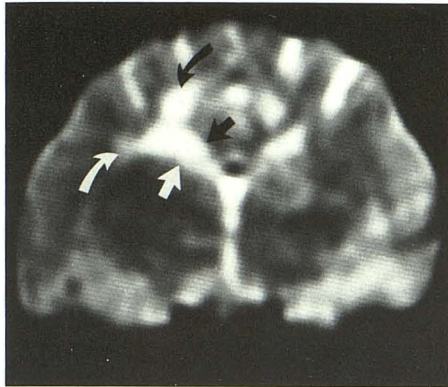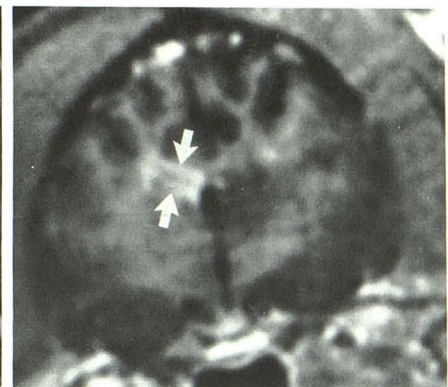
Fig. 3.—MR image of cat B 8 months after irradiation. High signal on T2-weighted image is seen both periventricularly (*straight arrows*) and extending superiorly and laterally from ventricles (*curved arrows*). SE 2000/100.

Fig. 4.—T2-weighted image of cat B before (*A*) and after (*B*) Gd shows enhancement of periventricular lesion only (*arrows*). Blood-brain barrier breakdown in area of radiation necrosis. IR 2000/800.

Fig. 5.—*A*, Magnification ×12 of histologic coronal section of cat B shows right lateral ventricle (*asterisk*), necrotic periventricular white-matter lesions (*wide arrow*), and subcortical demyelinated white-matter lesions (*thin arrows*). Increased vascularity (*arrowhead*) is also present.

B, Magnification ×192 of necrotic subependymal tissue (outlined by *arrows*).
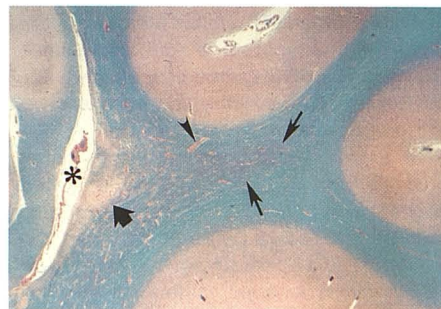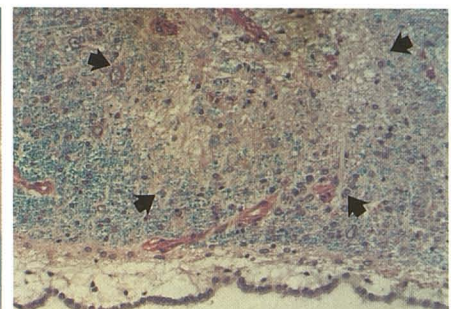
damaged blood-brain barrier [3]. Long TE SE images have been shown to be quite sensitive to a wide degree of CNS pathology manifested by an increase in signal intensity and due to increased water. Tumor, edema, infarcts, demyelinated multiple sclerosis plaques, and infection have all been seen as areas of high signal [3, 12].

Although only two of six animals in our series developed lesions, the radiologic-pathologic correlation was precise. Cat A displayed high-signal abnormality in the white matter corresponding to a region of demyelination that did not enhance with Gd-DTPA. Our work with Gd-DTPA in an animal model of demyelination and in patients with multiple sclerosis [13] suggests that lack of enhancement indicates absence of active inflammation. An acute radiation-induced demyelinating lesion might show enhancement, as do active multiple sclerosis plaques [13].

After intravenous Gd-DTPA, cat B manifested enhancement on T1-weighted images in areas corresponding to histologically proven radiation necrosis. Cat B also demonstrated adjacent nonenhancing lesions in white-matter tracts that correlated pathologically with edema and pallor of the myelin, increased vascularity, and swollen astrocytes. This high signal extending into the white matter on T2-weighted images in cat

B probably represents vasogenic edema from the adjacent necrotic tissue around the right lateral ventricle, the corpus callosum, and the fornix. Areas of radiation necrosis are often surrounded by vasogenic edema radiating into adjacent white-matter tracts [4].

Swollen astrocytes and neovascularity also suggest some direct radiation injury to the nonenhancing region of high signal. The absence of demyelinated axons and macrophages suggests this injury occurs early and is possibly a precursor to active demyelination. It is uncertain whether lesions at this stage are reversible [4].

Our results indicate that radiation produces focal regions of noninflammatory demyelination, edema, and necrosis, which have a similar appearance on T2-weighted images. Gd-DTPA may be useful in separating necrosis from the other two entities. Defining the spectrum of MR changes in the brain after irradiation has important implications in the diagnosis and treatment of CNS neoplasia.

REFERENCES

1. Dooms GC, Hecht S, Brant-Zawadzki M, et al. Brain radiation lesions: MR imaging. *Radiology* **1986**;158:149–155
2. Curnes JT, Laster DW, Ball MR, Moody DM, Witcofski RL. Magnetic resonance imaging of radiation injury to the brain. *AJNR* **1986**;7:389–394
3. Grossman RI, Joseph PM, Wolf G, et al. Experimental intracranial septic infarction: magnetic resonance enhancement. *Radiology* **1985**:155:649–653
4. Rubin P, Casarett GW. Central nervous system. In: *Clinical radiation pathology*, vol. 2. Philadelphia: Saunders, **1968**;609–661
5. Lampert PW, Davis RL. Delayed effects of radiation on the human CNS—"Early" and "late" delayed reactions. *Neurology* **1964**;14:912–917
6. Mikhael MA. Radiation necrosis of the brain: correlation between computed tomography, pathology, and dose distribution. *J Comput Assist Tomogr* **1978**;2:71–80
7. Mikhael MA. Radiation necrosis of the brain: correlation between patterns on computed tomography and dose of radiation. *J Comput Assist Tomogr* **1979**;3(2):241–249
8. Rottenberg DA, Chernik NK, Deck MDF, et al. Cerebral necrosis following radiotherapy of extracranial neoplasms. *Ann Neurol* **1977**;1:339–357
9. Zeman W, Samorajski T. Effects of irradiation on the nervous system. In: Berdjis CC, ed. *Pathology of irradiation.* Baltimore: Williams & Wilkins, **1971**:213–277
10. Courville CB, Myers RO. The process of demyelination in the central nervous system. II. Mechanism of demyelination and necrosis of the cerebral centrum incident to x-radiation. *J Neuropathol Exp Neurol* **1958**;17:158–173
11. Caveness WF. Experimental observations: delayed necrosis in normal monkey brain. In: Gilbert HA, Kagan AR, eds. *Radiation damage to the nervous system.* New York: Raven Press, **1980**
12. Bydder GM, Steiner RE, Young IR, et al. Clinical NMR imaging of the brain: 140 cases. *AJNR* **1982**;3:459–480
13. Grossman RI, Gonzalez FS, Atlas SW, et al. Multiple sclerosis: gadolinium enhancement in MR imaging. *Radiology* **1986**;161:721–725